Jurnal Teknologi

Full paper

Discrete Element Modelling of Complex Failure Mechanism at Quarry Slope

Rini A. Abdullah,* Mohd For Mohd Amin, Ahmad S.A. Rashid, S.M. Yahya

Department of Geotechnics & Transportation, Faculty of Civil Engineering, Universiti Teknologi Malaysia, 81310 UTM Johor Bahru, Johor Malaysia

*Corresponding author: asnida@utm.my

Article history

Received: 17 August 2014
Received in revised form:
17 November 2014
Accepted: 24 December 2014

Graphical abstract

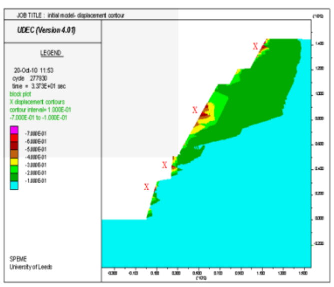

Abstract

Road cutting, open pit mining, quarrying and various other constructions in hilly terrain demand special attention in terms of slope stability. The analysis of slope stability is of great significance not only for ensuring safe design of excavated slope, but also for preventing potential hazards. This research was undertaken to identify the controlling parameters affecting the slope instability. As the rock slope behaviour is mostly governed by discontinuities, discontinuum numerical technique such as Discrete Element Method (DEM) which has the ability to address discontinuity controlled instability is well suited for this case. This study investigated the failure pattern and its responsible factors leading to failure of a slope at a slate quarry situated in Wales, United Kingdom as a case study. The research work consisted of field investigation, laboratory experiments and parametric analysis by powerful and renowned distinct element computational tool Universal Discrete Element Code (UDEC). Evidence showed that complex failure mechanism involving distinct planar sliding surface along with block-flexural toppling contributed to the instability at the studied slate quarry. Dip of discontinuity, presence of water, weathering state and slope angle were the significant factors found in this study to have profound impact on controlling rock slope instability. The modelling results also indicated that the influence of structurally dipping at 78° of cleavage in slate and the water filling in the crack which developed excess water pressure have triggered the failure.

Keywords: Discrete element method; UDEC; rock slope; block-flexural toppling

Abstrak

Kerja-kerja yang melibatkan pemotongan cerun batuan seperti bagi pembinaan jalan raya, perlombongan, kuari dan lain-lain pembinaan memerlukan perhatian khusus dari sudut kestabilan cerun. Analisis kestabilan cerun bukan sahaja mengakibatkan impak yang besar bagi memastikan keselamatan rekabentuk cerun, malahan juga bagi mencegah kemungkinan bencana. Kajian ini bertujuan mengenal pasti parameter penting yang memberi pengaruh kepada ketidakstabilan cerun. Oleh kerana cerun batuan sangat dipengaruhi oleh sifat ketidakselanjaran itu sendiri, maka teknik berangka tak berhubung iaitu Kaedah Unsur Diskret yang berupaya menangani ketakselanjaran yang mengakibatkan ketidakstabilan cerun digunakan. Kajian ini dilakukan ke atas sifat kegagalan dan faktor-faktor yang menyebabkan kegagalan cerun di sebuah kuari yang terletak di Wales, United Kingdom. Kajian ini melibatkan penyiasatan lapangan, kerja-kerja makmal dan analisis berparameter dengan menggunakan perisian Universal Discrete Element Code (UDEC). Hasil kajian mendapati bahawa mekanisma kegagalan yang kompleks yang melibatkan gelongsoran dan blok-lenturan jatuhan menyebabkan ketidakstabilan pada cerun di kuari tersebut. Kemiringan ketakselanjaran, kehadiran air, tahap luluhawa dan sudut potongan cerun merupakan faktor utama yang dikenalpasti sebagai penyebab utama kepada ketidakstabilan cerun tersebut. Hasil daripada pemodelan juga menunjukkan bahawa sudut ketidaselanjaran berstruktur pada 78° dan kehadiran air di dalam retakan telah menyebabkan peningkatan tekanan air yang berlebihan telah mencetuskan kegagalan cerun ini.

Kata kunci: Kaedah unsur diskret; Universal Discrete Element Code (UDEC); cerun batuan; blok-lenturan jatuhan

1.0 INTRODUCTION

In rock slope stability, there is no single parameter which dominates the rock slope behaviour. Rather, a combination of properties determines the slope behaviour [1-13]. Therefore, a robust type of analysis is required to represent the behaviour of rock slopes. Broad selections of analysis types are available, which includes limit equilibrium, kinematics and probability approaches and now more recently, the numerical types of analysis which covers finite element and discrete element methods [14-20]. The discrete element method which allowed modelling and analysis of the rock mass as a discontinuum is considered be an alternative way of understanding rock slope behaviour. It also has found to give good agreement with the real-world conditions [21-25]. Since the rock masses consist of an assemblage of blocks with discontinuities, it would be reasonable to analyse and predict the stability of the rock slope using this method. Discontinuous 'distinct block' numerical calculations can model the discontinuities and calculate the behaviour of a rock mass in all detail, if necessary property data are available [26].

2.0 FAILED QUARRY SLOPE

The quarry located near Bethesda in north Wales (Fig. 1). It was once reputed to be the world's largest slate quarry. The slate is known as Llanberis slate of Early Cambrian age (Fig. 2). The development of a slaty cleavage is a direct result of realignment, through orientation and or re-crystallisation. This preferred alignment of platy minerals accounts for cleavage in slate, which gives pronounced anisotropy [27].

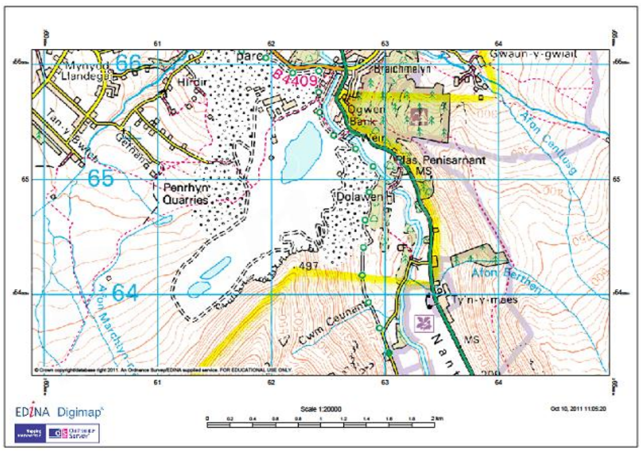

Figure 1 Location of slate quarry [28]

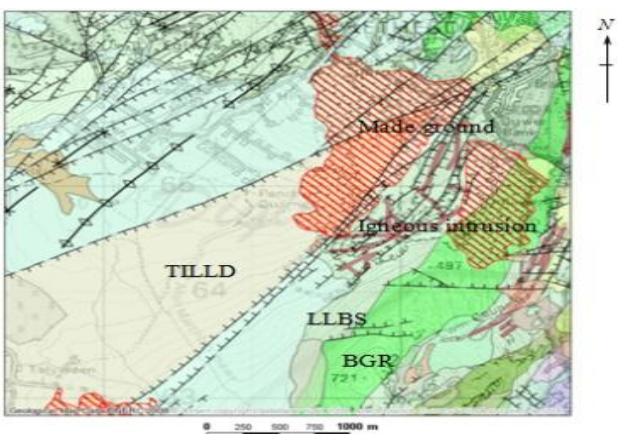

Legend:	Rock unit	Age
	Till Devensian (TILLD)	Devensian
	Llanberis Slates Formation (LLBS)	Early Cambrian
	Bronllwyd Grit Formation (BGR)	Late Cambrian

Figure 2 Geology of slate quarry [28]

Figure 3 Failure occurred in October, 2008

Figure 4 Flexural toppling and overturning at rear of failure

Figure 5 Cracks monitoring point at the rear of instability

The south-eastern faces have been the site of a series of large historic slope failures in both the North and South Quarries over the past 100 years. Following a significant failure in the North Quarry in 1989 this area was closed and the workings were then concentrated in the South Quarry. The most recent instability occurred overnight on 2nd October 2008, with a secondary movement reported to have occurred during 5th October 2008, see (Fig. 3-5).

3.0 DISCRETE ELEMENT METHOD (DEM)

The slope was modelled by the DEM in Universal Discrete Element Code (UDEC). The aims of numerical experiments in DEM are to investigate the failure mechanism and monitor the slope behaviour.

In general, the slope consists of five benches giving an overall height of c. 150m and slope angle of 52°. Full persistence is assumed on cleavage, since it appeared to be the most critical joint for slope instability. Meanwhile persistency for the other joint sets is achieved from back analysis of the slope itself [29]. The engineering properties have been gathered through laboratory work (Table 1).

Table 1 Engineering properties of slate

Test type	Parameter	Value		
Intact rock properties (Cleavage direction = 78°)				
Density test	Density (Gg/m^3)	0.0027		
Triaxial test	E (GPa)	62.3		
	υ	0.34		
	c (MPa)	25		
	ϕ_b (°)	52		
UCS	UCS (MPa)	146		
Brazilian test	Tensile strength (MPa)	6.6		
Discontinuity properties		Cleavage	Joint	Fault
Profilometer	JRC	2	4	6
Schmidt hammer	JCS (MPa)	130	130	130
Direct shear test	ϕ_r dry (°)	32	32	32
	Aperture (mm)	0.05	0.12	0.15
	Jk_n (MPa/m)	48660	22614	20887
	Jk_s (MPa/m)	18022	8376	8223

Notation:						
	E	=	Young's modulus	JCS	=	Joint compressive strength
	υ	=	Poison's ratio	ϕ_b	=	Basic friction angle
	c	=	Cohesion	ϕ_r	=	Residual friction angle
	UCS	=	Unconfined compressive strength	Jk_n	=	Joint normal stiffness
	JRC	=	Joint roughness coefficient	Jk_s	=	Joint shear stiffness

4.0 CONSTITUTIVE MODEL

Since slate is an anisotropic material, the Ubiquitous joint model (UJM) has been applied to describe the strength of the intact rock instead of the conventional Mohr-Coulomb (MC) failure criterion. The UJM accounts for the orientation of weakness in the MC model. Here, yield may occur in either the solid or along the weakness plane, or both, depending on the stress state, the orientation of the weakness planes and the material properties. It should be noted that this model does not account for the specific location of a weakness plane, only an orientation [30]. Additional input parameters should be assigned in the model properties which are dip of the discontinuity (78°) and discontinuity friction angle (32°).

The Barton-Bandis (BB) joint model has been applied to the discontinuity. This criterion describes the strength of a discontinuity surface and it depends on the combined effects of the surface roughness, rock strength at the surface, the applied normal stress and the amount of shear displacements. A series of comparative models between MC and BB joint models for the slope have been previously published [29]. The BB criterion is also found to be better in describing the joint behaviour because of its non-linearity [17, 21]. Data for the BB joint model has been given in Table 1.

4.1 Initial Model

The initial model was built based on the pre-failure survey without considering of any tension crack developed due to the presence of water. The excavation stage is simulated to generate the most appropriate in situ stress condition. Five excavation stages have been performed on the model with regards to the slope benches. Higher density of discontinuity was assigned around the slope face for modelling purposes. Any small released rock block near the slope face will be also removed to avoid a misleading result.

4.2 Adding Complexity to the Model

The complexities of the model are add-ons, i.e. by introducing the tension crack, increase in level of the water table and applying water pressure in the tension crack; they are added subsequently into the model. The tension crack is applied by increasing the aperture width [31]. Since there is no information for the measurement of the water table, by referring to Figure 4, which shows water form at the base of the slope, so, it is assumed that the water table to be at 1/3 and 2/3 of the slope height. Therefore, the water table is applied to the slope at 50m and then increased to 100m from the toe by using a command of the pore pressure boundary. The calculation of water pressure for the BB joint model can be performed through the aperture properties assigned [31].

■5.0 MODELLING RESULTS AND DISCUSSIONS

The strain criterion approach has been considered as an additional means to assess the stability performance of open pit slopes. In real slopes, the strain approach is based on the correlation value from target prism monitoring data, whereas in numerical modelling, the calculation of strain is obtained from the given block deformation value. Slope strain is as in Equation 1. The suggested strain threshold value is shown in Table 2 [32].

$$\varepsilon = \frac{\Delta\chi}{H} * 100 \tag{1}$$

Where, $\Delta\chi$ is the maximum deformation of the slope and H is the total height of the slope.

Table 2 Suggested threshold strain levels [32]

Highwall stability stage	Threshold strain level (%)
Tension cracks	~ 0.1
Progressive movements	~ 0.6
Collapse	> 2.0

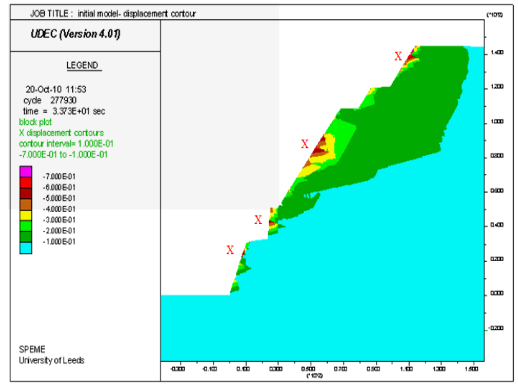

Figure 6 Location (X) of tension crack in slope model

It was found from Figure 6, that the maximum displacement was 0.7m which was located at a few locations at the top, middle and bottom of the slope (marked with X). This gives the slope strain of 0.47%, which reflects the development of a tension crack (Table 2).

Once greater complexity was introduced into the model, it was discovered that with the presence of tension cracks and water table, the percent strain for the slope was increased to 3% and slope fell into the collapse category.

In general, the slope undergoes a complex type of failure. From the displacement vectors, the slope displayed a complex type of failure which consists of toppling between the cleavages and sliding along joints (Fig. 7).

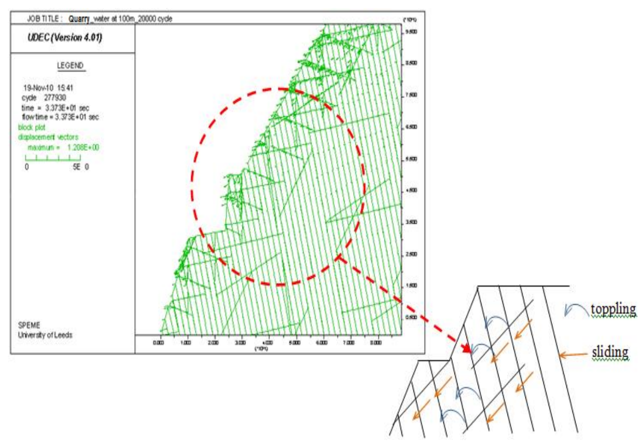

Figure 7 Vectors show the direction of block movement

It is believed that block flexural toppling was the mode of failure. Block flexural toppling is bounded by the basal failure plane and the movement is also influenced by displacement on the cross joint. As can be seen in Figure 8, the failure depth is at about 15m. At the toe, joints start to slip and block rotation can also be observed.

Further movement of the slope takes place when a water table was present at a depth of 100m. The water that filled in the crack pushed the block further and the slope failed with a maximum displacement of 3m. Shearing of blocks which involves the rotation is illustrated in Figure 9. It shows that the larger block at (A) slides and rotated a higher degree thus acts as a chisel causing the block at the front to slide along the daylighting joint. Further toppling also triggers the cleavage to compress and bend. Opening up the cleavage is due to tensile failure.

UDEC output	Description

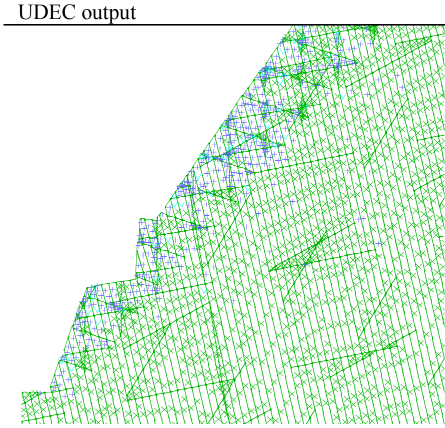

Slip joint for 20,000 cycles

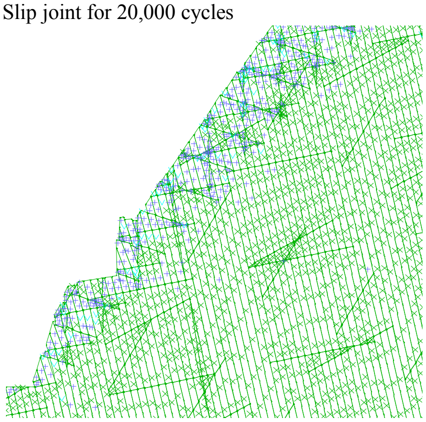

Slip joint for 60,000 cycles

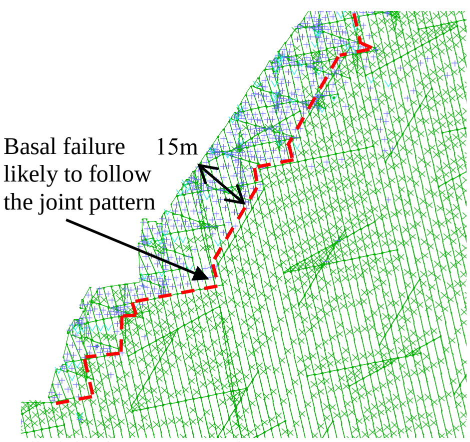

Slip joint for 100,000 cycles

The weakness point in slate is through its cleavage. Blue crosses (+) in the figure shows the slip that developed through the cleavage. This increases over the number of numerical cycles. The movement in the slope with cycle time is demonstrated. Toppling also involved shearing between the cleavage fractures, and created a basal failure plane. The basal failure is identical to the flexural toppling type of failure. However, it was discovered at the end of the cycle, that the slip between the cleavage has stopped in the joint and follows the joint pattern. Further slip on the cleavage has caused the columns to bend and compress the columns in the front, where it creates space due to tensile failure. The movement allows for block rotation and further toppling takes place.

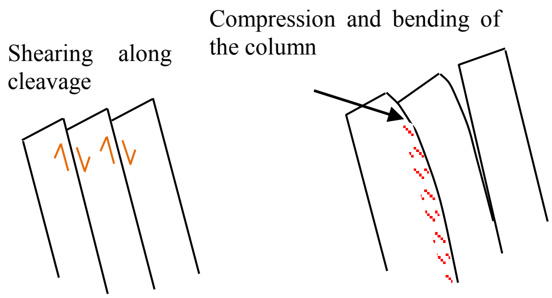

Figure 8 Slip along the cleavage creates a basal failure that is identical to flexural toppling failure

UDEC output	Description
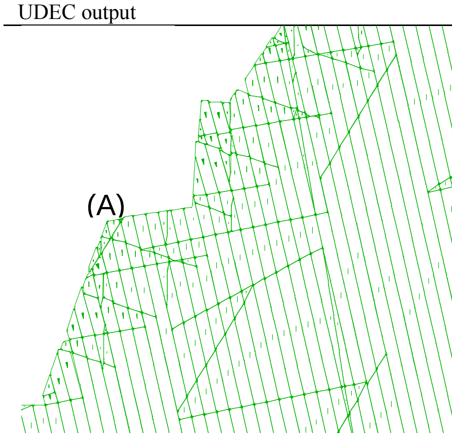 Block rotation for 20,000 cycles	At the same time, sliding occurred through the daylighting joint. The block at location (A), experienced sliding and rotating due to the smaller block size. It acted like a chisel; digging and pushing the block at the front to move toward the daylighting joint. 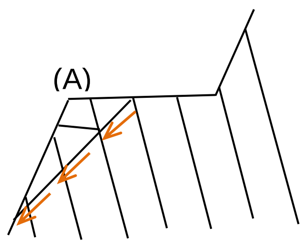 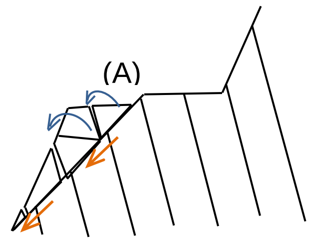
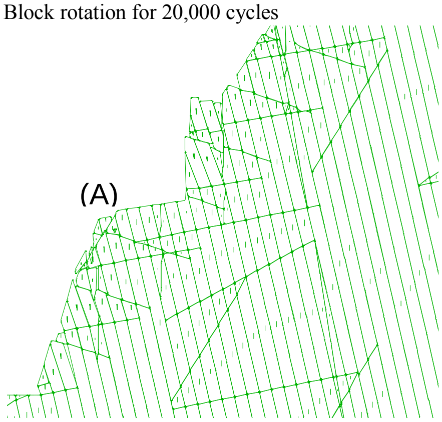 Block rotation for 60,000 cycles	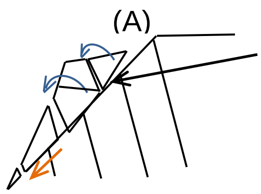 Due to sliding and rotation the block chiselled up the front block to move forward.
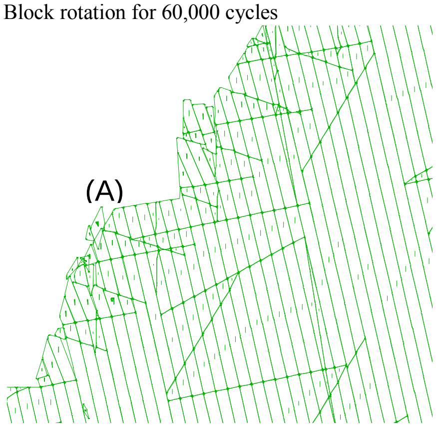 Block rotation for 100,000 cycles	

Figure 9 Shear failure involving block rotation

This mechanism was found to explain the pattern of slope movement, which was the objective of the modelling. It also confirms the failure observed on site. There are two main aspects in the instability which are water and tension crack. The collapse of the slope took place after a period of heavy rainfall (Fig. 10). The graph showed that September experienced the heaviest rainfall event without the failure. The implication is that, the slope is generally close to limiting equilibrium, which may be disturbed by heavy rain. This was evidence of movement with the development of tension cracks in the field before the main failure occurred (Fig. 5). Then, the opening of a tension crack being filled with water and triggering the failure at a later date.

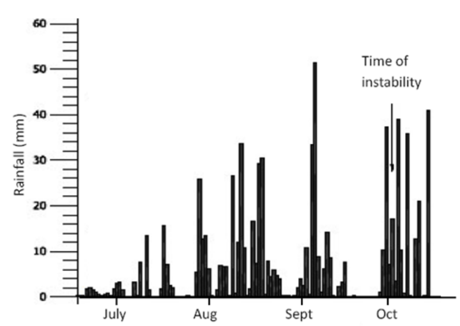

Figure 10 Rainfall data event at the quarry slope

■6.0 SENSITIVITY ANALYSIS OF SLOPE

Then, sensitivity analyses has been carried out related to the weathering grade and the analysis on reduction of slope angle will also be carried out to see the effects of slope geometry on behaviour. The analysis was performed by varying the value of one factor while all other factors remained constant. The analyses were carried out to assess the slope behaviour when weathering takes place. The weathering was assessed through the reduction of the JCS value (Table 3) [33]. For simplification of analysis, the weathering was assumed to be constant throughout the discontinuities (Table 4). In addition, the assessment on the slope angle was also carried out to observe the effects of slope geometry contributing to the instability of the slope. The overall slope angle was reduced from 52° to 35° (Fig. 11). This includes flattening the individual slope at about 50°compared to initial individual slope angle that range from 55° – 85°. All the models were tested against four slope condition, i.e. 1) initial model, 2) presence of tension crack, 3) presence of tension crack with water table at 50m and 4) presence of tension crack with water table at 100m.

Table 3 Description of weathering state [33]

Weathering state	UCS/JCS ratio
Fresh to Slightly weathered	UCS/JCS < 1.2
Moderately weathered	1.2 < UCS/JCS < 2
Weathered	UCS/JCS > 2

Table 4 Sensitivity analysis for Weathering grade (W)

Weathering grade	Fresh (UCS/JCS=1.1)			Moderately weathered (UCS/JCS=1.6)			Weathered (UCS/JCS=2.4)		
	Cleavage	Joint	Fault	Cleavage	Joint	Fault	Cleavage	Joint	Fault
JCS (MPa)	130	130	130	90	90	90	60	60	60
UCS (MPa)	146	146	146	146	146	146	146	146	146

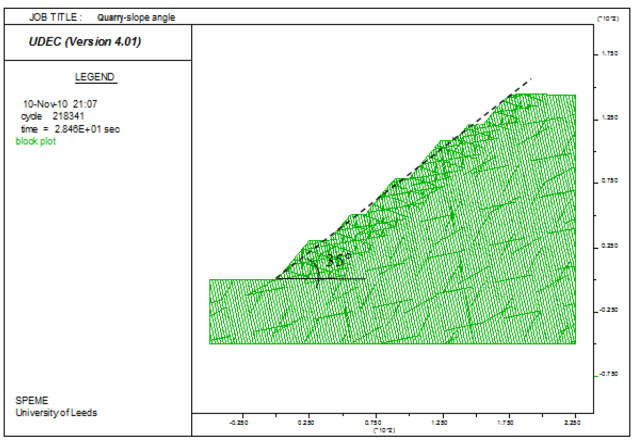

Figure 11 UDEC model for Slope Angle (SA) analysis with overall slope angle=35°

■7.0 RESULTS AND DISCUSSION

Figures 12 and 13 show the results of the sensitivity analysis carried out on weathering grade and slope angle respectively. It can be seen that, for the initial model, with increasing of weathering grade (fresh to weathered), strain increased steadily from 0.47% (fresh) to 0.80% (moderately weathered) and 1.33% (weathered). This upward pattern of strain is directed to all slope conditions i.e. slope with tension crack and water. In general, the fresh rock slope only collapses once it is modelled with 100m height of water table. Meanwhile, for a moderately weathered rock slope it was observed to collapse once the water table was introduced and for weathered rock slope, it was demonstrated that the slope itself will collapse with only the presence of a tension crack in the slope.

It is evident that, the more weathered the rock mass, the more unstable the slope is. This can be explained by changing the discontinuity strength. With lower JCS value, the asperities are more likely to be sheared off and damaged rather than overriding. Unlike overriding the asperities, shearing of the asperities will be encouraged by reduction of JCS and therefore promote movement.

With the presence of the tension crack, strain increased to almost double for all weathering states. Opening the tension crack eliminates the rock to rock contact and reduces shear strength between the discontinuities. Strain continues to increase when the water was introduced for 50m of the slope height. Thus, with the presence of water at 100m, it does promote further movements of the slope.

What happened is, the water pressure reduces the shear strength, and this condition has been observed from the laboratory tests [34]. The water also generates a force to push the block further. Water may also wash away the filling material and left no rock to rock contact, and this will demolish the shear strength and consequently, increased the instability.

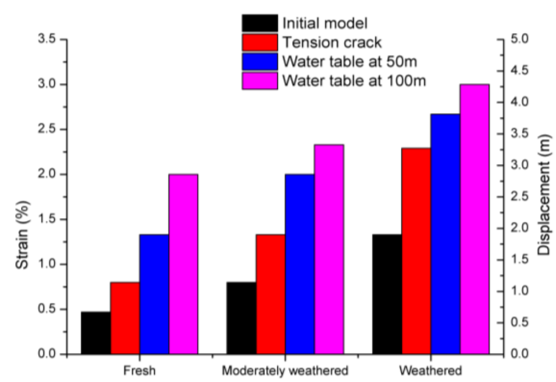

Figure 12 Sensitivity analysis for weathering grade for the slope

For the analysis of the effect on slope angle, the results show that by flattening the slope, the strain is reduced for all slope conditions. In this case, the slope is found to be stable except that the tension crack was developed for the slope that was modelled with a water table at 100m height.

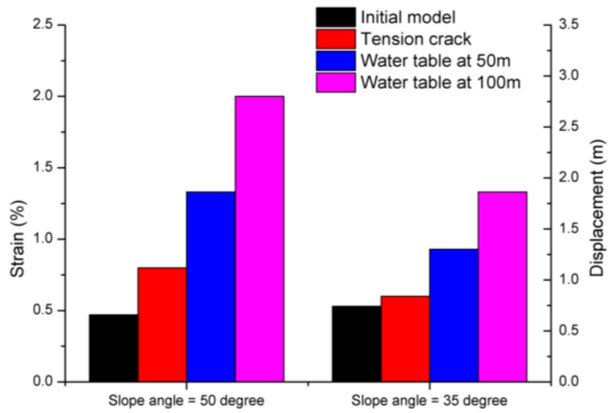

Figure 13 Sensitivity analysis for the slope angle

8.0 CONCLUSION

UDEC modelling provides a useful insight into the rock slope failure mechanism at failed quarry slope, where evidence of a complex failure mechanism has contributed to the instability. Generally, this failure was dominant by a structurally dipping at 78° of cleavage in slate. The water then triggered the failure when it fills in the crack and developed the water pressure that pushed the block movement. This confirmed that dip of discontinuity and water are the significant parameter in controlling the rock slope behaviour at the failed slope. Further sensitivity analysis has confirmed the influence of water to the rock slope instability. The analyses also demonstrate the effect of discontinuity orientation to the slope behaviour. More study is needed to incorporate with other parameters that may contribute to the rock slope behaviour such as block size and shape, joint roughness and excavation method.

Acknowledgement

The authors would like to acknowledge Dr. D. Jameson, GWP Consultants, UK for suggesting this as a project, Dr. Mark Christianson from Itasca Consulting Group for his guidance with UDEC and Dr. Robert Fowell and Dr. William Murphy from University of Leeds for their supervision.

References

[1] Deere, D.U., A.J. Hendron, F.D. Patton and E.J. Cording. 1967. Design of surface and near surface construction in rock. *Proc. 8th U.S. Symp. Rock Mech*. New York: AIME. 237–302.

[2] Wickham, G.E., H.R. Tiedemann, and E.H. Skinner. 1972. Support determination based on geological prediction. *Proc. North American Rapid Excav. Tunnelling Conf*. New York: AIME. 43–64.

[3] Bieniawski, Z.T. 1989. *Engineering Rock Mass Classifications: A Complete Manual For Engineers And Geologists In Mining, Civil And Petroleum Engineering*. New York: John Wiley and Sons.

[4] Barton, N., R. Lien, and J. Lunde.1974. Engineering classification of rock masses for the design of tunnel support. *Rock Mechanics*. 6(4): 189–236.

[5] Hoek, E. and E.T. Brown. 1997. Practical Estimates of rock mass strength. *Int. J. Rock Mech. Min. Sci*. 34(8): 1165–186.

[6] Palmstrøm, A. 1996. Characterizing rock masses by RMi for use in practical rock engineering. *Tunnelling and Underground Space Technology*. 11(2): 175–188.

[7] E. Romana, M., J.B. Serón, and E. Montalar. 2003. SMR Geomechanics classifcation: Application, experience and validation. *Proceedings of the 10th Congress of the International Society for Rock Mechanics: ISRM 2003 - Technology Roadmap for Rock Mechanics, South African Institute of Mining and Metallurgy*. 1–4.

[8] Laubscher, D.H. 1977. Geomechanics classification of jointed rock masses - mining application. *Trans. Instn. Min. Metall. (Sect. A: Min. Industry)*. 86: A1–A8.

[9] Sonmez, H. and R. Ulusay. 1999. Modifications to the geological strength index (GSI) and their applicability to stability of slopes. *Int. J. Rock Mech. Min. Sci*. 36: 743-760.

[10] Hudson, J.A. and J.P. Harrison. 1992. A new approach to studying complete rock engineering problems. *Quarterly Journal of Engineering Geology*. 25: 93–105.

[11] Hack, R., D. Price, and N. Rengers. 2003. A new approached to rock slope stability - a probability classification (SSPC). *Bulletin of Engineering Geology and the Environment*. 62(2): 167–184.

[12] Nicholson, D.T. 2004. Hazard assessment for progressive, weathering related breakdown of excavated rockslopes. *Quarterly Journal of Engineering Geology and Hydrogeology*. 37: 327–346.

[13] Pantelidis, L. 2010. An alternative rock mass classification system for rock slopes. *Bulletin of Engineering Geology and the Environment*. 69(1): 29–39.

[14] Li, X. 2007. Finite element analysis of slope stability using a nonlinear failure criterion. *Computer and Geotechnics*. 34(3): 127–136.

[15] Alejano, L.R., A.M. Ferrero, P. Ramírez-Oyanguren, M. I. Álvarez Fernández. 2011. Comparison of limit equilibrium, numerical and physical models of wall slope stability. *Int. J. Rock Mech. Min. Sci*. 48(1): 16–26.

[16] Cheng, Y.M., T. Lansivaara, and W.B. Wei. 2007. Two-dimensional slope stability analysis by limit equilibrium and strength reduction methods. *Computers and Geotechnics*. 34(3): 137–150.

[17] Bhasin, R. and K. Hoeg. 1998. Parametric study for a large cavern in jointed rock using a distinct element model (UDEC - BB). *Int. J. Rock Mech. Min. Sci.* 35(1): 17–29.

[18] Brideau, M.A., D. Stead, and R. Couture. 2006. Structural and engineering geology of East Gate Landslide, Purcell Mountains, British Columbia, Canada. *Engineering Geology*. 84(3/4)): 183–206.

[19] McCollough, M.F. 1993. Numerical modelling with UDEC of the footwall slope of Aznalcollar mine, Southern Spain. *M.Sc. Thesis, Department of Mining & Mineral Engineering, University of Leeds, United Kingdom*. 143.

[20] Preh, A. and R. Poisel 2004. A UDEC model for "kink-band slumping" type failures of rock slopes. *Proc. of the 1st Int. UDEC/3DEC Symp., Bochum, Germany, Balkema: Numerical Modelling of Discrete Materials in Geotechnical Engineering, Civil Engineering & Earth Sciences*. London: Taylor & Francis Group. 243–247

[21] Choi, S.O. and S.K. Chung. 2004. Stability analysis of jointed rock slope with the Barton-Bandis constitutive model in UDEC. *Int. J. Rock Mech. Min. Sci*. 41(3): 1–6.

[22] Allison, R.J. and O.G. Kimber. 1998. Modelling failure mechanism to explained rock slope change along the Isle of Purbeck Coast, UK. *Earth Surface Processes and Landforms*. 23(8): 731–750.

[23] Mitani, Y., T. Esaki, and Y. Cai. 2004. A numerical study about flexure toppling phenomenon on rock slopes. *Proc. of the 1st Int. UDEC/3DEC Symp., Bochum, Germany, Balkema: Numerical Modelling of Discrete Materials in Geotechnical Engineering, Civil Engineering & Earth Sciences*. London: Taylor & Francis Group. 235–241.

[24] Bhasin, R. and A.M. Kaynia. 2004. Static and dynamic simulation of a 700-m high rock slope in western Norway. *Engineering Geology*. 71: 213–226.

[25] Tosney, J.R., D. Milne, A.V. Chance and F. Amon. 2004. Verification of a large scale slope instability mechanism at Highland Valley Copper. *International Journal of Mining, Reclamation and Environment*. 18(4): 273–288.

[26] Hack, R. 2002. An evaluation of slope stabiliy classification. *Proceedings of ISRM International Symposium, EUROCK 2002: Rock Engineering for Mountainous Regions*. 3–32.

[27] Bell, F.G. 1981. *Engineering Properties of Soils and Rocks*. London: Butterworths. 149.

[28] Digimap. 2011. Retrieved October 10, 2011, from http://digimap.edina.ac.uk/digimap/home

[29] Abdullah, R.A., R.J. Fowell, and W. Murphy. 2010. Selecting shear strength models for joints - experience with modelling of complex rock slope failure in UDEC. *Proceedings of the European Rock Mechanics Symposium, EUROCK 2010: Rock Mechanics in Civil and Environmental Engineering*. Switzerland: Taylor & Francis Group. 543–546.

[30] Itasca. 2004. *UDEC Version 4.01*. Minneapolis, Minnesota, USA: Itasca Consulting Group, Inc.

[31] Bhasin, R. 2008. Barton Bandis joint model in UDEC. Personal communication.

[32] Brox, D. and W. Newcomen. 2003. Utilizing strain criteria to predict highwall stability performance. *Proceedings of the 10th Congress of the International Society for Rock Mechanics: ISRM 2003–Technology Roadmap for Rock Mechanics, South African Institute of Mining and Metallurgy*. 157–161.

[33] Bandis, S.C., A.C. Lumsden, and N.R. Barton. 1983. Fundamentals of rock joint deformation. *Int. J. Rock Mech. Min. Sci*. 20(6): 249–268.

[34] Abdullah, R.A. 2011. Development of a slope classification system with particular reference to shallow rock slope failure. *Ph.D. Thesis, School of Process, Environmental and Materials Engineering, University of Leeds, United Kingdom*. 210.